Probing the space-time geometry around black hole candidates with the resonance models for high-frequency QPOs and comparison with the continuum-fitting method

Cosimo Bambi

Arnold Sommerfeld Center for Theoretical Physics,
Ludwig-Maximilians-Universität München,
D-80333 Munich, Germany

E-mail: Cosimo.Bambi@physik.uni-muenchen.de

Abstract. Astrophysical black hole candidates are thought to be the Kerr black hole predicted by General Relativity. However, in order to confirm the Kerr-nature of these objects, we need to probe the geometry of the space-time around them and check that observations are consistent with the predictions of the Kerr metric. That can be achieved, for instance, by studying the properties of the electromagnetic radiation emitted by the gas in the accretion disk. The high-frequency quasi-periodic oscillations observed in the X-ray flux of some stellar-mass black hole candidates might do the job. As the frequencies of these oscillations depend only very weakly on the observed X-ray flux, it is thought they are mainly determined by the metric of the space-time. In this paper, I consider the resonance models proposed by Abramowicz and Kluzniak and I extend previous results to the case of non-Kerr space-times. The emerging picture is more complicated than the one around a Kerr black hole and there is a larger number of possible combinations between different modes. I then compare the bounds inferred from the twin peak high-frequency quasi-periodic oscillations observed in three micro-quasars (GRO J1655-40, XTE J1550-564, and GRS 1915+105) with the measurements from the continuum-fitting method of the same objects. For Kerr black holes, the two approaches do not provide consistent results. In a non-Kerr geometry, this conflict may be solved if the observed quasi-periodic oscillations are produced by the resonance $\nu_\theta : \nu_r = 3 : 1$, where ν_θ and ν_r are the two epicyclic frequencies. It is at least worth mentioning that the deformation from the Kerr solution required by observations would be consistent with the one suggested in another recent work discussing the possibility that steady jets are powered by the spin of these compact objects.

Contents

1 Introduction **1**

2 Characteristic orbital frequencies **3**

3 Resonance models **6**
3.1 Parametric resonances 7
3.2 Forced resonances 8
3.3 Keplerian resonances 8

4 The observed twin peak high-frequency QPOs in BH candidates **8**
4.1 GRO J1655-40 9
4.2 XTE J1550-564 9
4.3 GRS 1915+105 11

5 Discussion and conclusions **13**

1 Introduction

In 4-dimensional General Relativity, uncharged black holes (BHs) are described by the Kerr solution, which is completely specified by two quantities: the mass, M, and the spin parameter, $a_* = J/M^2$, where J is the spin angular momentum, of the compact object[1] [1–3]. A fundamental limit for a Kerr BH is the bound $|a_*| \le 1$, which is the condition for the existence of the event horizon. For $|a_*| > 1$, there is no horizon and the Kerr metric describes the gravitational field around a naked singularity, which is forbidden by the Weak Cosmic Censorship Conjecture [4].

It is widely believed that the final product of the gravitational collapse is a Kerr BH, as follows from a body of analytical and numerical studies [4–8] (but see [9–12] and references therein). Astronomers have also discovered several good astrophysical candidates [13]. In particular, we have about twenty stellar-mass BH candidates in X-ray binary systems. For the time being, we can only get a robust measurement of the mass of these objects. That is possible by studying the orbital motion of the stellar companion. The latter is relatively far from the compact object and its trajectory is well described by Newtonian mechanics. In this way, we can estimate the mass of the compact object without any assumption about its nature. As these masses turn out to exceed 3 $M_\odot$ (the maximum mass for a neutron or quark star assuming no phase transition to exotic forms of matter at densities below the nuclear one [14, 15]), these objects are thought to be Kerr BHs, as they cannot be explained otherwise without introducing new physics.

In order to confirm the Kerr-nature of the known astrophysical BH candidates, we need to probe the geometry of the space-time around them and check if it is consistent with the predictions of General Relativity [16]. That can be achieved in a number of way. In the case of stellar-mass BH candidates, we may get information on the geometry of the space-time around these objects by studying the thermal spectrum of their accretion disk during the high-soft state [17, 18], by the analysis of relativistic lines [19, 20], and possibly even by

[1]Throughout the paper, I use units in which $G_{\rm N} = c = 1$.

measuring the power of their jets [21, 22]. If the stellar companion is a radio pulsar, its orbital motion can be accurately tracked and we can get information about the nature of the BH candidate [23]. Ground-based gravitational wave detectors are supposed to be able to observe BH quasi-normal modes (QNMs) in a near future and, since the ones of a Kerr BH depend only on M and J, the possible detection of at least three modes can test the Kerr-nature of the source [24]. Other approaches can instead be used only to probe the geometry of the space-time around super-massive BH candidates in galactic nuclei [25–34].

Another promising tool to test the nature of stellar-mass BH candidates is represented by the so-called quasi-periodic oscillations (QPOs). The X-ray power density spectra of some low-mass X-ray binaries show some peaks; that is, there are QPOs in the X-ray flux[2] [36]. These features can be observed in systems with both BH candidates and neutron stars and the frequencies of these oscillations are in the range 0.1-10^3 Hz. High-frequency QPOs in BH candidates ($\sim$40-450 Hz) are particularly interesting, as they depend only very weakly on the observed X-ray flux and for this reason it is thought they are determined by the metric of the space-time rather than by the properties of the accretion flow. If that is correct, high-frequency QPOs can be used to probe the geometry around stellar-mass BH candidates. For the time being, however, the exact physical mechanism responsible for the production of the high-frequency QPOs is not known and several different scenarios have been proposed, including hot-spot models [37, 38], diskoseismology models [39–42], and resonance models [43–46]. In these models, the frequencies of the QPOs are directly related to the characteristic orbital frequencies of test-particles.

The possibility of using QPOs to test the strong gravitational field around stellar-mass BH candidates has been already studied [47–49]. In [47, 48], the authors consider a very specific case, the braneworld BH metric proposed in [50], in which the geometry of the space-time is fairly similar to the one of an electrically charged BH of General Relativity. Let us notice, however, that this solution may be strongly constrained by current Solar System experiments (but only if the Birkhoff's Theorem holds). In Ref. [49], the authors study QPOs in a quasi-Kerr metric, valid only for small spin parameters and small deviations from the Kerr solution. In this paper, I study the phenomenon in a quite generic stationary and axisymmetric non-Kerr background and I find a much more complicated picture. In particular, the possibility of the existence of vertically unstable orbits, absent in the Kerr background, allows for a larger number of possible combinations between different modes. I then consider the scenario of resonance models proposed by Abramowicz and Kluzniak [43–46], mainly motivated by the observed 3:2 double peak high-frequency QPOs in micro-quasars, and I compare theoretical predictions with observational data. Lastly, I compare these results with the measurements inferred from the continuum-fitting method of the same objects. In the Kerr case, this approach is equivalent to the comparison of the spin measurements from high-frequency QPOs and continuum-fitting method and the question of consistency of the two techniques has been discussed in Ref. [51]. While high-frequency QPOs and continuum-fitting method do not seem to provide consistent results for Kerr BHs, the conflict may be solved if the space-time around BH candidates deviates from the Kerr solution.

The content of the paper is as follows. In Sec. 2, I discuss the characteristic orbital frequencies of test-particles in the Johannsen-Psaltis (JP) metric [52], which is a stationary and axisymmetric space-time with very generic deviations from the Kerr background. In Sec. 3, I apply the results of the previous section to the resonance models. In Sec. 4, I consider

[2] QPOs have been observed even in the spectra of super-massive BH candidates, see e.g. Ref. [35].

the observational data of the three stellar-mass BH candidates with observed twin peak high-frequency QPOs and with a measurement of the mass. These objects are GRO J1655-40, XTE J1550-564, and GRS 1915+105. Fortunately, for them we have also measurements of the thermal spectrum of their disk during the high-soft state and I can thus compare the allowed region in the plane spin parameter-deformation parameter inferred from the QPOs with the one determined from the continuum-fitting method. Discussion and conclusions are in Sec. 5.

2 Characteristic orbital frequencies

Let us now focus on equatorial orbits, as the accretion disk around BH candidates is normally expected to lie on the equatorial plane of the system. Circular orbits of test-particles are characterized by three frequencies: the Keplerian frequency $\nu_{\rm K}$ (which is the inverse of the orbital period), the radial epicyclic frequency ν_r (the frequency of radial oscillations around the mean orbit), and the vertical epicyclic frequency ν_θ (the frequency of vertical oscillations around the mean orbit). These three frequencies depend on the geometry of the space-time and on the radius of the orbit. While they are defined as the characteristic frequencies of the orbital motion for a free particle, there is a direct relation between these frequencies and the ones of the oscillation modes of the fluid accretion flow.

In Newtonian gravity with potential $V = -M/r$, the three characteristic frequencies has the same value:

$$\nu_{\rm K} = \nu_r = \nu_\theta = \frac{M}{r^{3/2}} \, . \tag{2.1}$$

They are plotted as a function of the radial coordinate in the top left panel of Fig. 1.

In General Relativity, a key-ingredient is the existence of the innermost stable circular orbit (ISCO). In the Schwarzschild metric, the ISCO radius is $r_{\rm ISCO} = 6M$. In the Kerr background, the ISCO radius decreases (increases) as the spin parameter a_* increases for corotating (counterrotating) orbits. For a maximally rotating Kerr BH ($a_* = 1$), the ISCO radius is respectively $r_{\rm ISCO} = M$ for the corotating case and $r_{\rm ISCO} = 9M$ for the counterrotating one. Circular orbits with radii smaller than $r_{\rm ISCO}$ are radially unstable. That means the radial epicyclic frequency ν_r reaches a maximum at some radius $r_{\rm max} > r_{\rm ISCO}$ and then vanishes at the ISCO. Keplerian and vertical epicyclic frequencies are instead defined up to the innermost circular orbit (also called photon orbit). Circular orbits with radius smaller than the one of the photon orbit do not exist. In the Kerr metric, $\nu_\theta > \nu_r$, while, for corotating orbits, $\nu_{\rm K} \ge \nu_\theta$. $\nu_{\rm K}$, ν_r, and ν_θ in the Schwarzschild space-time are shown in the top right panel of Fig. 1. The Kerr cases with spin parameter $a_* = 0.9$ and 0.998 and for corotating orbits are shown respectively in the bottom left and bottom right panels of Fig. 1.

In the case of a generic non-Kerr background, the picture is more complicated. The most important difference is that the ISCO radius may be determined by the stability of the orbit along the vertical (instead of the radial) direction [17, 53]. In some metrics, there is also the possibility of the existence of one or more regions of stable circular orbits inside the ISCO and therefore with smaller radii. These regions of stable orbits are separated by a gap from the "traditional" ISCO; the details depend on the specific metric, but usually they do not play any physical role, as they can accept only particles with energy higher than the one at the ISCO. In what follows, I will consider the JP metric [52], as it seems to include all the relevant features of a generic space-time deviating from the Kerr solution. While several authors have

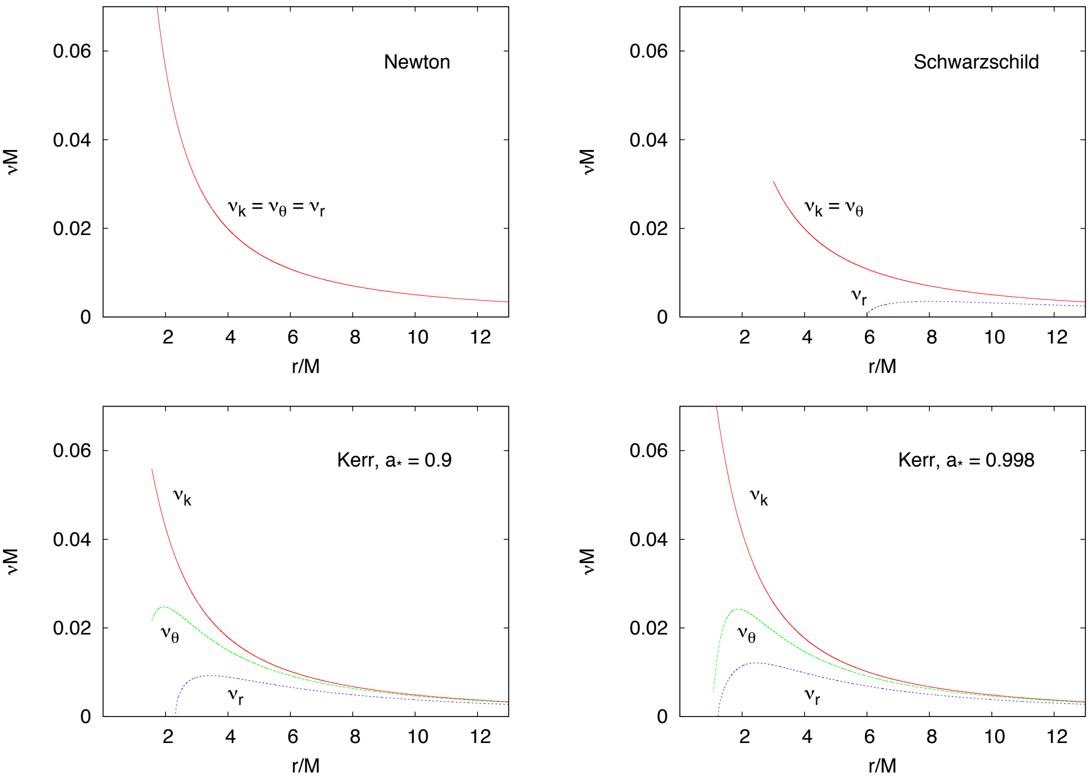

Figure 1. Profiles of the Keplerian frequency $\nu_{\rm K}$, the radial epicyclic frequency ν_r, and the vertical epicyclic frequency ν_θ in Newtonian gravity with potential $-M/r$ (top left panel), in the Schwarzschild space-time (top right panel), and in the Kerr space-time with spin parameter $a_* = 0.9$ (bottom left panel) and $a_* = 0.998$ (bottom right panel). See text for details.

proposed specific alternatives to Kerr BHs for the astrophysical BH candidates (like Q-stars, gravastars, or non-Kerr BHs solutions of specific and theoretically motivated extensions of General Relativity), here the choice of the JP metric with a single deformation parameter can be motivated as follows. The aim of this work is not to test a specific theoretical model and to determine/constrain its parameters, but to investigate in a model-independent way possible deviations from the Kerr geometry of the space-time around astrophysical BHs. The JP metric is used to perform a null-experiment: it is like the Kerr metric with a deformation parameter measuring possible deviations from the Kerr solution and the spirit is to determine this deformation parameter and check it is zero. Current and near-future data are indeed not so good to map the space-time around a BH candidate and a single deformation parameter is used to figure out if the gravitational force is stronger or weaker than the one around a Kerr BH with the same mass and spin. Actually, the typical situation is even worse and with one measurement we can only infer one parameter: if we assume the Kerr background, we find the spin a_* (but we find a wrong value if the object is not a Kerr BH), if we have also a deformation parameter, we constrain some combination of a_* and of the deformation parameter. With two independent measurements, we can determine both the spin and the deformation parameter. The choice of the JP metric should thus be understood with this spirit and it makes sense if it is used to check if the geometry of the space-time is described by the Kerr solution, not to investigate the actual nature of the compact object or the exact

deviations from the Kerr background.

In Boyer-Lindquist coordinates, the JP metric is given by the line element

$$
\begin{aligned}
ds^2 = & -\left(1-\frac{2Mr}{\Sigma}\right)(1+h)\,dt^2 + \\
& +\frac{\Sigma(1+h)}{\Delta + a^2 h \sin^2\theta}dr^2 + \Sigma\,d\theta^2 - \frac{4aMr\sin^2\theta}{\Sigma}(1+h)\,dt\,d\phi + \\
& + \left[\sin^2\theta\left(r^2+a^2+\frac{2a^2Mr\sin^2\theta}{\Sigma}\right) + \frac{a^2(\Sigma+2Mr)\sin^4\theta}{\Sigma}h\right]d\phi^2\,, \qquad (2.2)
\end{aligned}
$$

where $a = a_* M$, $\Sigma = r^2 + a^2\cos^2\theta$, $\Delta = r^2 - 2Mr + a^2$, and

$$
h = \sum_{k=0}^{\infty}\left(\epsilon_{2k} + \frac{Mr}{\Sigma}\epsilon_{2k+1}\right)\left(\frac{M^2}{\Sigma}\right)^k . \qquad (2.3)
$$

The JP metric has an infinite number of deformation parameters ϵ_i and the Kerr solution is recovered when all the deformation parameters are set to zero. However, in order to reproduce the correct Newtonian limit, we have to impose $\epsilon_0 = \epsilon_1 = 0$, while ϵ_2 is strongly constrained by Solar System experiments [52]. In this paper, I consider a simple case with a sole deformation parameter ϵ_3 and $\epsilon_i = 0$ for $i \neq 3$. A different choice of the deformation parameter, like ϵ_4 or ϵ_5 instead of ϵ_3, would not change the qualitative features of our non-Kerr metric, as well as our results and conclusions [54].

In a generic stationary, axisymmetric, and asymptotically flat space-time, the characteristic orbital frequencies can be computed numerically as follows. The line element of the space-time can be written in the canonical form

$$
ds^2 = g_{tt}dt^2 + g_{rr}dr^2 + g_{\theta\theta}d\theta^2 + 2g_{t\phi}dtd\phi + g_{\phi\phi}d\phi^2\,, \qquad (2.4)
$$

where the metric components are independent of the t and ϕ coordinates, which implies the existence of two constants of motion: the conserved specific energy at infinity, E, and the conserved z-component of the specific angular momentum at infinity, L_z. This fact allows to write the t- and ϕ-component of the 4-velocity of a test-particle as

$$
u^t = \frac{E g_{\phi\phi} + L_z g_{t\phi}}{g_{t\phi}^2 - g_{tt}g_{\phi\phi}}\,, \qquad u^\phi = -\frac{E g_{t\phi} + L_z g_{tt}}{g_{t\phi}^2 - g_{tt}g_{\phi\phi}}\,. \qquad (2.5)
$$

From the conservation of the rest-mass, $g_{\mu\nu}u^\mu u^\nu = -1$, we can write

$$
g_{rr}\dot{r}^2 + g_{\theta\theta}\dot{\theta}^2 = V_{\rm eff}(r,\theta,E,L_z)\,, \qquad (2.6)
$$

where $\dot{r} = u^r = dr/d\lambda$, $\dot{\theta} = u^\theta = d\theta/d\lambda$, λ is an affine parameter, and the effective potential $V_{\rm eff}$ is given by

$$
V_{\rm eff} = \frac{E^2 g_{\phi\phi} + 2EL_z g_{t\phi} + L_z^2 g_{tt}}{g_{t\phi}^2 - g_{tt}g_{\phi\phi}} - 1\,. \qquad (2.7)
$$

Circular orbits on the equatorial plane are located at the zeros and the turning points of the effective potential: $\dot{r} = \dot{\theta} = 0$, which implies $V_{\rm eff} = 0$, and $\ddot{r} = \ddot{\theta} = 0$, requiring respectively

$\partial_r V_{\rm eff} = 0$ and $\partial_\theta V_{\rm eff} = 0$. From these conditions, one can obtain the Keplerian angular velocity $\Omega_{\rm K}$, E, and L_z of the test-particle:

$$\Omega_{\rm K} = \frac{d\phi}{dt} = \frac{-\partial_r g_{t\phi} \pm \sqrt{\left(\partial_r g_{t\phi}\right)^2 - \left(\partial_r g_{tt}\right)\left(\partial_r g_{\phi\phi}\right)}}{\partial_r g_{\phi\phi}} \,, \tag{2.8}$$

$$E = -\frac{g_{tt} + g_{t\phi}\Omega}{\sqrt{-g_{tt} - 2g_{t\phi}\Omega - g_{\phi\phi}\Omega^2}} \,, \tag{2.9}$$

$$L_z = \frac{g_{t\phi} + g_{\phi\phi}\Omega}{\sqrt{-g_{tt} - 2g_{t\phi}\Omega - g_{\phi\phi}\Omega^2}} \,, \tag{2.10}$$

where in $\Omega_{\rm K}$ the sign $+$ is for corotating orbits and the sign $-$ for counterrotating ones. The Keplerian frequency is simply $\nu_{\rm K} = \Omega_{\rm K}/2\pi$. The orbits are stable under small perturbations if $\partial_r^2 V_{\rm eff} \le 0$ and $\partial_\theta^2 V_{\rm eff} \le 0$.

The radial and vertical epicyclic frequencies can be quickly computed by considering small perturbations around circular equatorial orbits, respectively along the radial and vertical direction. If δ_r and δ_θ are the small displacements around the mean orbit (i.e. $r = r_0 + \delta_r$ and $\theta = \pi/2 + \delta_\theta$), we find they are governed by the following differential equations

$$\frac{d^2\delta_r}{dt^2} + \Omega_r^2 \delta_r = 0 \,, \tag{2.11}$$

$$\frac{d^2\delta_\theta}{dt^2} + \Omega_\theta^2 \delta_\theta = 0 \,, \tag{2.12}$$

where [45]

$$\Omega_r^2 = -\frac{1}{2g_{rr}(u^t)^2}\frac{\partial^2 V_{\rm eff}}{\partial r^2} \,, \tag{2.13}$$

$$\Omega_\theta^2 = -\frac{1}{2g_{\theta\theta}(u^t)^2}\frac{\partial^2 V_{\rm eff}}{\partial \theta^2} \,. \tag{2.14}$$

The radial epicyclic frequency is thus $\nu_r = \Omega_r/2\pi$ and the vertical one is $\nu_\theta = \Omega_\theta/2\pi$. The radial profile of the three characteristic orbital frequencies in the JP background with spin parameter $a_* = 0.8$ and four different values of the deformation parameter ϵ_3 is shown in Fig. 2.

3 Resonance models

In four stellar-mass BH candidates, we observe two high-frequency QPOs. It is remarkable that in all the four cases the ratio of the two frequencies is 3:2, suggesting a strong correlation between them. Possible theoretical models should thus be able to explain this feature. The resonance models proposed by Abramowicz and Kluzniak [43–46] seem to be quite appealing from this point of view. In Eqs. (2.11) and (2.12), the radial and the vertical modes are decoupled. However, it is natural to expect that in a more realistic description there are non-linear effects coupling the two epicyclic modes. In this case, the equations can be written as

$$\frac{d^2\delta_r}{dt^2} + \Omega_r^2 \delta_r = \Omega_r^2 F_r\left(\delta_r, \delta_\theta, \frac{d\delta_r}{dt}, \frac{d\delta_\theta}{dt}\right) \,, \tag{3.1}$$

$$\frac{d^2\delta_\theta}{dt^2} + \Omega_\theta^2 \delta_\theta = \Omega_\theta^2 F_\theta\left(\delta_r, \delta_\theta, \frac{d\delta_r}{dt}, \frac{d\delta_\theta}{dt}\right) \,, \tag{3.2}$$

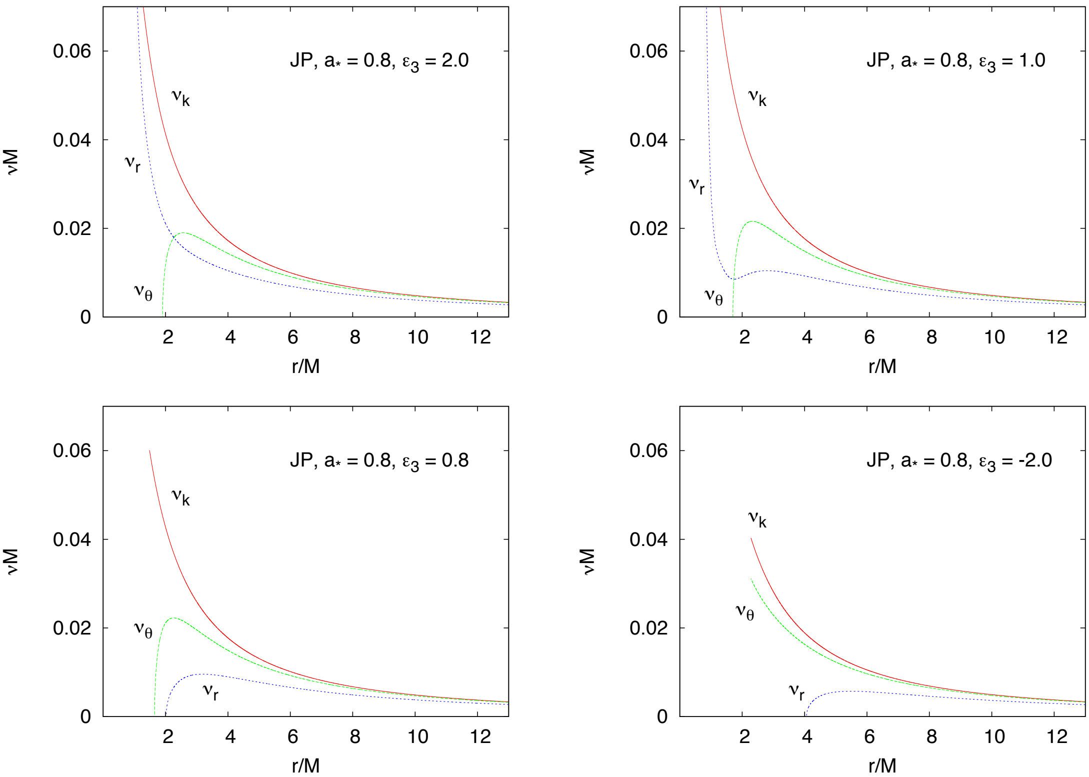

Figure 2. Profiles of the Keplerian frequency $\nu_{\rm K}$, the radial epicyclic frequency ν_r, and the vertical epicyclic frequency ν_θ in the JP space-time with spin parameter $a_* = 0.8$ and deformation parameter $\epsilon_3 = 2.0$ (top left panel), $\epsilon_3 = 1.0$ (top right panel), $\epsilon_3 = 0.8$ (bottom left panel), and $\epsilon_3 = -2.0$ (bottom right panel). See text for details.

where F_r and F_θ are some functions that depend on the specific properties of the accretion flow. If we knew the details of the physical mechanisms of the accretion process, we could write the explicit form of these two functions and solve the system. Unfortunately, that is not the case. The strategy is therefore to guess possible properties and consequences of these equations and see if they can be fitted in a plausible physical scenario.

3.1 Parametric resonances

A simple but interesting scenario is to imagine that vertical oscillations are governed by the Mathieu equation [44, 46]:

$$\frac{d^2\delta_\theta}{dt^2} + \Omega_\theta^2 \delta_\theta = -\Omega_\theta^2 h \cos(\Omega_r t)\delta_\theta \, , \tag{3.3}$$

which corresponds to the case with $F_r = 0$ and $F_\theta = -\delta_r\delta_\theta$: the solution of Eq. (3.1) is simply $\delta_r = h\cos(\Omega_r t)$ and so we obtain Eq. (3.3). The Mathieu equation describes indeed a parametric resonance with

$$\frac{\Omega_r}{\Omega_\theta} = \frac{2}{n} \, , \qquad n = 1, 2, 3, ... \tag{3.4}$$

The resonance is stronger for smaller values of n. In the Kerr background, $\nu_\theta > \nu_r$, and therefore the resonance $n = 3$ can naturally explain the observed 3:2 ratio if the upper

frequency $\nu_{\rm U}$ is associated with ν_θ and the lower frequency $\nu_{\rm L}$ with ν_r. In the JP space-time with $\epsilon_3 > 0$, $\nu_\theta > \nu_r$ may not be true (depending on the value of the spin parameter), as the ISCO may be determined by the orbital stability along the vertical direction. In this case, the resonances $n = 1$ and 2 may be exited and indeed be stronger than the resonance $n = 3$. For $n = 1$, the observed 3:2 ratio might be interpreted as $\nu_{\rm U} = \nu_r + \nu_\theta$ and $\nu_{\rm L} = \nu_r$. For $n = 2$, as $\nu_{\rm U} = 3\nu_r = 3\nu_\theta$ and $\nu_{\rm L} = 2\nu_r = 2\nu_\theta$.

3.2 Forced resonances

The equation for vertical oscillations may also include a forced resonance, in which the force frequency is equal to the one of the radial oscillations [46]:

$$\frac{d^2\delta_\theta}{dt^2} + \Omega_\theta^2\delta_\theta + [\text{non linear terms in } \delta_\theta] = h(r)\cos(\Omega_r t)\,. \tag{3.5}$$

The non-linear terms allow resonant solutions for δ_θ, with frequencies like

$$\Omega_- = \Omega_\theta - \Omega_r\,, \tag{3.6}$$

$$\Omega_+ = \Omega_\theta + \Omega_r\,. \tag{3.7}$$

The observed 3:2 ratio may be explained with $\nu_\theta : \nu_r = 3 : 1$ ($\nu_{\rm U} = \nu_\theta$ and $\nu_{\rm L} = \nu_-$) or with $\nu_\theta : \nu_r = 2 : 1$ ($\nu_{\rm U} = \nu_+$ and $\nu_{\rm L} = \nu_\theta$). In non-Kerr backgrounds with vertically unstable ISCO, we have also the possibility that $\nu_r > \nu_\theta$ and therefore, at least in principle, resonances like $\nu_\theta : \nu_r = 1 : 2$ and $\nu_\theta : \nu_r = 1 : 3$ may exist.

3.3 Keplerian resonances

The possibility of a coupling between Keplerian and radial epicyclic frequencies might exist, even if it seems to be less theoretically motivated than the one in which the coupling is between the two epicyclic oscillations. The simplest combinations are: $\nu_{\rm K} : \nu_r = 3 : 2$ ($\nu_{\rm U} = \nu_{\rm K}$ and $\nu_{\rm L} = \nu_r$), $\nu_{\rm K} : \nu_r = 3 : 1$ ($\nu_{\rm U} = \nu_{\rm K}$ and $\nu_{\rm L} = 2\nu_r$), and $\nu_{\rm K} : \nu_r = 2 : 1$ ($\nu_{\rm U} = 3\nu_r$ and $\nu_{\rm L} = \nu_{\rm K}$). For non-Kerr backgrounds, there are no new phenomena with respect to the standard Kerr framework, as $\nu_{\rm K} > \nu_r$ is still true.

4 The observed twin peak high-frequency QPOs in BH candidates

In four stellar-mass BH candidates we observe two high-frequency QPOs in the X-ray flux and the ratio between the upper and the lower frequency turns out to be $\nu_{\rm U} : \nu_{\rm L} = 3 : 2$. For three of these objects, we have also a dynamical measurement of the mass, which allows us to use the observed twin peak high-frequency QPOs to test their nature (supposing we have the exact model for the production of QPOs). These three objects are listed in Tab. 1, with their mass M and the observed upper and lower high-frequency QPOs $\nu_{\rm U}$ and $\nu_{\rm L}$. Regardless of the specific resonance model and the microphysics responsible for it, the resonance paradigm requires that the upper and the lower frequencies have the form

$$\nu_{\rm U} = m_1\nu_r + m_2\nu_\theta\,, \tag{4.1}$$

$$\nu_{\rm L} = n_1\nu_r + n_2\nu_\theta\,. \tag{4.2}$$

where m_1, m_2, n_1, and n_2 are integer (and likely as small as possible) numbers. For Keplerian resonance models, $\nu_{\rm U}$ and $\nu_{\rm L}$ have clearly the form $\nu_{\rm U} = m_1\nu_{\rm K} + m_2\nu_r$ and $\nu_{\rm L} = n_1\nu_{\rm K} + n_2\nu_r$. Assuming the JP background with deformation parameter ϵ_3, we can compare the theoretical predictions with the observed $\nu_{\rm U}$ and $\nu_{\rm L}$ for any BH candidate and define an allowed region on the plane spin parameter-deformation parameter for any specific set of $\{m_1, m_2, n_1, n_2\}$.

BH binary	$M/M_\odot$	$\nu_{\rm U}$/Hz	$\nu_{\rm L}$/Hz	References
GRO J1655-40	6.30 ± 0.27	450 ± 3	300 ± 5	[55]
XTE J1550-564	9.1 ± 0.6	276 ± 3	184 ± 5	[56]
GRS 1915+105	14.0 ± 4.4	168 ± 3	113 ± 5	[36]

Table 1. Stellar-mass BH candidates in binary systems with a measurement of the mass and two observed high-frequency QPOs.

4.1 GRO J1655-40

GRO J1655-40 is the object with the best measurements for both the mass of the BH candidate and the two high-frequency QPOs, see Tab. 1. If we assume $\nu_{\rm U}$ and $\nu_{\rm L}$ are the result of the coupling between the radial and the vertical epicyclic oscillations, we can compute ν_r and ν_θ from Eqs. (2.13) and (2.14), consider a particular choice of $\{m_1, m_2, n_1, n_2\}$, and eventually find the allowed region on the plane spin parameter-deformation parameter on the base of the observed $\nu_{\rm U}$ and $\nu_{\rm L}$. Considering only the uncertainty on the mass M and neglecting the one in $\nu_{\rm U}$ and $\nu_{\rm L}$, the allowed region for some different choices of $\{m_1, m_2, n_1, n_2\}$ is shown in Figs. 3 and 4 (solid red curves)[3]. Fig. 5 shows the radial profiles of ν_r and ν_θ for two JP space-times with $\epsilon_3 = 8.0$, one with $a_* = 0.5$ and the other one with $a_* = 0.2$. In the former case, the condition $\nu_\theta : \nu_r = 3 : 2$ is satisfied at two radii and even the case $\nu_\theta : \nu_r = 2 : 3$ is possible. In the second example, we have $\nu_\theta : \nu_r = 3 : 2$ only at a single value of the radial coordinate and no $\nu_\theta : \nu_r = 2 : 3$.

As we can see, there is a degeneracy between the spin parameter a_* and the deformation parameter ϵ_3. This is the typical situation we find when we relax the Kerr BH hypothesis and we allow for non-vanishing deviations from the Kerr solution. In order to break this degeneracy, we need to use an independent constraint on a_* and ϵ_3. For instance, we can use the one coming from the analysis of the thermal spectrum of the accretion disk of GRO J1655-40 during the soft-high state. This technique is called continuum-fitting method [59, 60], its validity is supported by a number of observational and theoretical studies [61], and its extension to non-Kerr background is discussed in [17, 21, 22]. In Figs. 3 and 4, the region allowed by the continuum-fitting method is delimited by the dashed green line[4].

We can repeat the same exercise to the cases with coupling between Keplerian and radial epicyclic frequencies. The simplest combinations are $\nu_{\rm K} : \nu_r = 3 : 2$, $3 : 1$, and $2 : 1$. Fig. 6 shows the allowed regions in the plane spin parameter-deformation parameter, with the green dashed line still representing the bound coming from the continuum-fitting method.

4.2 XTE J1550-564

For GRO J1655-40, the resonance models considered in the previous subsection and the continuum-fitting method seem to provide consistent results only for $\nu_\theta : \nu_r = 3 : 1$ and $\nu_{\rm K}$:

[3] When we constrain a_* and ϵ_3, we cannot restrict our study to the region $|a_*| \le 1$, as this bound is justified only for Kerr BHs [6, 7]. In the case of non-Kerr objects, the issue of the instability depends on the details of the structure of the object and on the gravity theory, while the creation of a very compact object with $|a_*| > 1$ is possible (in the specific case of the JP space-time, at least for $\epsilon_3 < 0$), as shown in [34, 57, 58].

[4] The constraints coming from the continuum-fitting method for GRO J1655-40, XTE J1550-564, and GRS 1915+105 and shown in this paper are taken from Ref. [21].

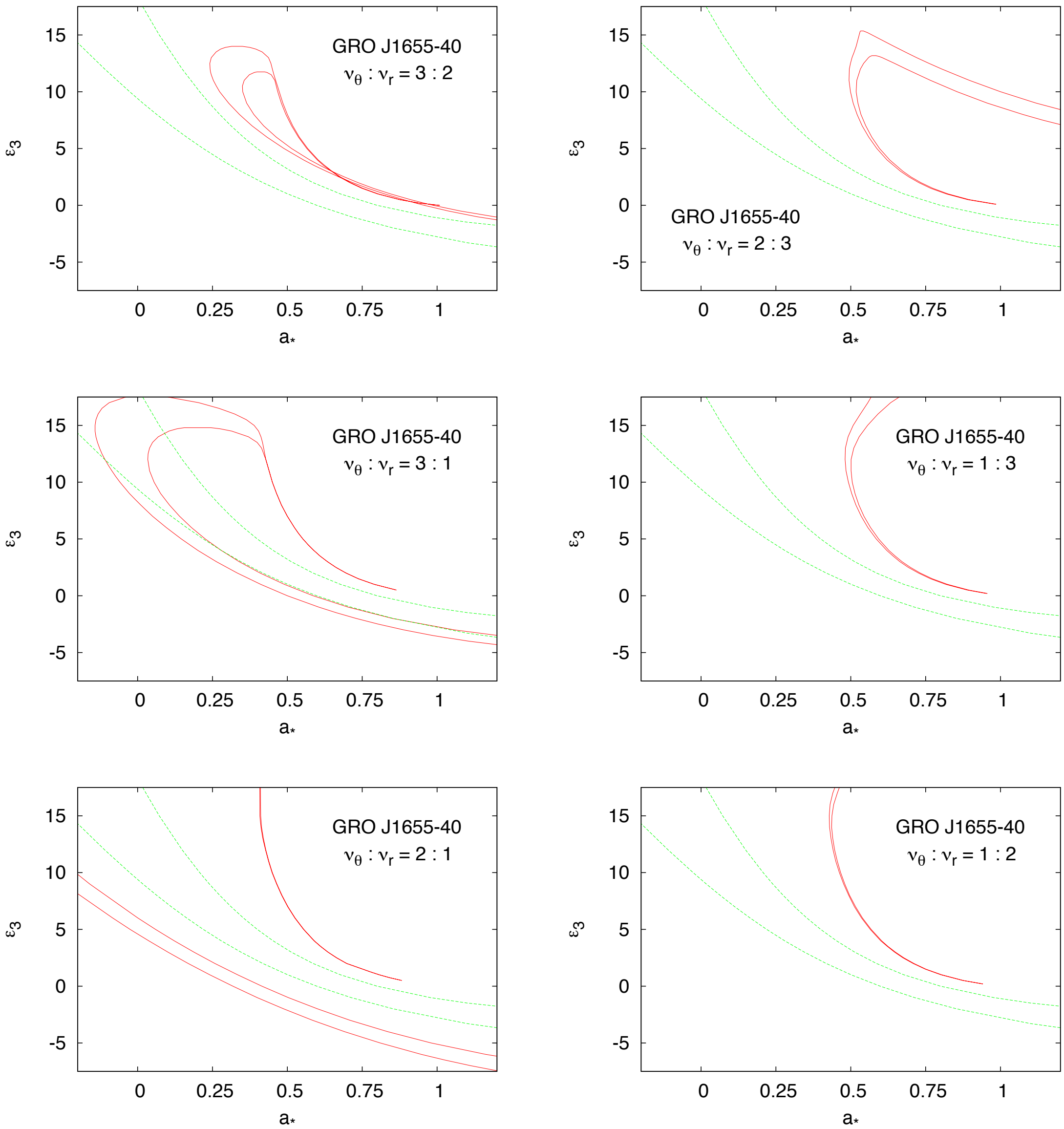

Figure 3. Constraints on the spin parameter a_* and the JP deformation parameter ϵ_3 for the BH candidate in the binary system GRO J1655-40 from resonance models of high-frequency QPOs (red solid curves) and the continuum-fitting method (green dashed curves). Top left panel: resonance $\nu_\theta : \nu_r = 3 : 2$ ($\nu_{\rm U} = \nu_\theta$ and $\nu_{\rm L} = \nu_r$). Top right panel: resonance $\nu_\theta : \nu_r = 2 : 3$ ($\nu_{\rm U} = \nu_r$ and $\nu_{\rm L} = \nu_\theta$). Central left panel: resonance $\nu_\theta : \nu_r = 3 : 1$ ($\nu_{\rm U} = \nu_\theta$ and $\nu_{\rm L} = \nu_\theta - \nu_r$). Central right panel: resonance $\nu_\theta : \nu_r = 1 : 3$ ($\nu_{\rm U} = \nu_r$ and $\nu_{\rm L} = \nu_r - \nu_\theta$). Bottom left panel: resonance $\nu_\theta : \nu_r = 2 : 1$ ($\nu_{\rm U} = \nu_\theta + \nu_r$ and $\nu_{\rm L} = \nu_\theta$). Bottom right panel: resonance $\nu_\theta : \nu_r = 1 : 2$ ($\nu_{\rm U} = \nu_r + \nu_\theta$ and $\nu_{\rm L} = \nu_r$). The resonances $\nu_\theta : \nu_r = 2 : 3$, $1 : 3$, and $1 : 2$ (right panels) are not allowed in a Kerr space-time.

$\nu_r = 3 : 1$ and for a non-vanishing deformation parameter $\epsilon_3 \sim 5 - 18$. For XTE J1550-564, in addition to these two possibilities, even the resonances $\nu_\theta : \nu_r = 2 : 1$ and $\nu_{\rm K} : \nu_r = 2 : 1$ would be in agreement with the results of the continuum-fitting method. However, in all the four cases the situation is like the one shown in Fig. 7 and the degeneracy between a_* and ϵ_3 is not broken.

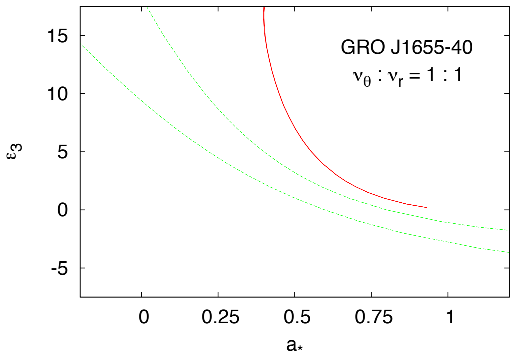

Figure 4. As in Fig. 3, for the resonance $\nu_\theta : \nu_r = 1 : 1$, which is not allowed around a Kerr BH.

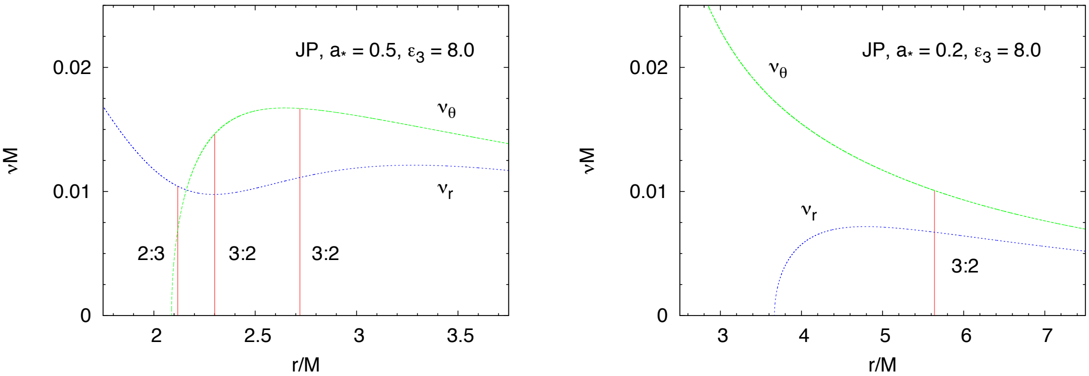

Figure 5. Profiles of the radial epicyclic frequency ν_r and of the vertical epicyclic frequency ν_θ in the JP space-time with deformation parameter $\epsilon_3 = 8.0$. Left panel: spin parameter $a_* = 0.5$; the resonance $\nu_\theta : \nu_r = 3 : 2$ is present at the radii $r/M = 2.30$ and 2.72, while the resonance $\nu_\theta : \nu_r = 2 : 3$ is at $r/M = 2.12$. Right panel: spin parameter $a_* = 0.2$; there is only one resonance $\nu_\theta : \nu_r = 3 : 2$, which takes place at the radius $r/M = 5.64$, and there is no resonance $\nu_\theta : \nu_r = 2 : 3$.

4.3 GRS 1915+105

For GRS 1915+105, the analysis of the thermal spectrum of the disk in the high-soft state in the Kerr background requires a quite high value of the spin parameter, $a_* > 0.97$ [62], which makes this objects very interesting[5]. If we consider the two resonances suggested by GRO J1655-40 (i.e. $\nu_\theta : \nu_r = 3 : 1$ and $\nu_{\rm K} : \nu_r = 3 : 1$), we get the two panels in Fig. 8. The resonance $\nu_\theta : \nu_r = 3 : 1$ (right panel in Fig. 8) may still produce consistent results between the two approaches, while the resonance $\nu_{\rm K} : \nu_r = 3 : 1$ may be ruled out.

Fig. 9 shows instead the resonance $\nu_\theta : \nu_r = 1 : 2$, which is allowed only for some values of a_* and ϵ_3 (see the right panel). In this case, QPOs and continuum-fitting method provide consistent measurements for non-vanishing ϵ_3. That is true even for other resonances with $\nu_r > \nu_\theta$, like $\nu_\theta : \nu_r = 1 : 3$ and $\nu_\theta : \nu_r = 1 : 1$ (not shown here). In a non-Kerr background we may thus have several resonances that exist only if the compact object rotates sufficiently

[5]As for GRO J1655-40 and XTE J1550-564, even in the case of GRS 1915+105 I am considering the measurement obtained by the Harvard group. However, for GRS 1915+105 other groups have found different values, see e.g. Ref. [63].

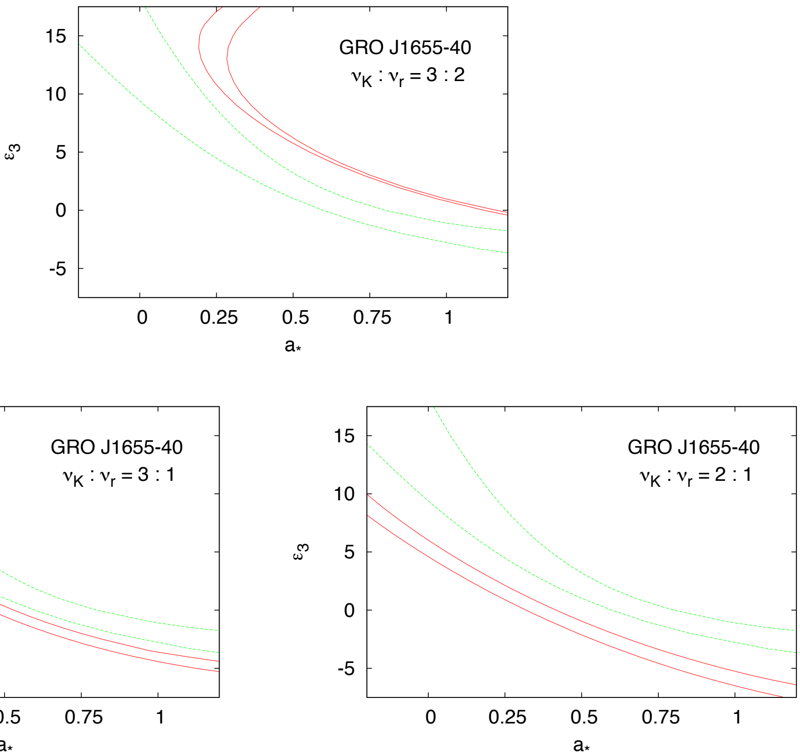

Figure 6. As in Fig. 3, in the case of Keplerian resonances: $\nu_{\rm K} : \nu_r = 3 : 1$ (top panel), $\nu_{\rm K} : \nu_r = 3 : 1$ (bottom left panel), and $\nu_{\rm K} : \nu_r = 2 : 1$ (bottom right panel).

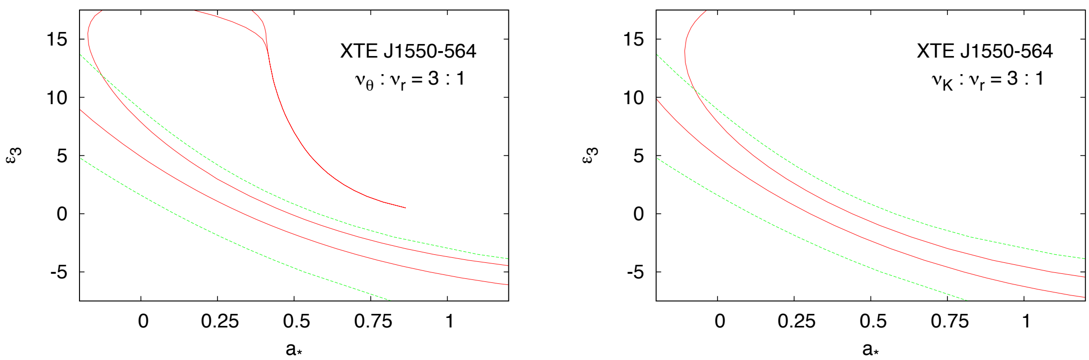

Figure 7. Constraints on the spin parameter a_* and the JP deformation parameter ϵ_3 for the BH candidate in the binary system XTE J1550-564 from resonance models of high-frequency QPOs (red solid curves) and the continuum-fitting method (green dashed curves). Resonances $\nu_\theta : \nu_r = 3 : 1$ (left panel) and $\nu_{\rm K} : \nu_r = 3 : 1$ (right panel).

fast.

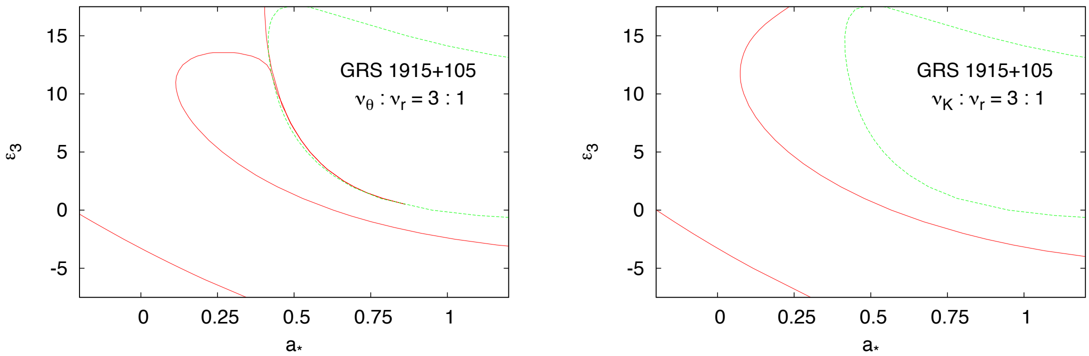

Figure 8. Constraints on the spin parameter a_* and the JP deformation parameter ϵ_3 for the BH candidate in the binary system GRS 1915+105 from resonance models of high-frequency QPOs (red solid curves) and the continuum-fitting method (green dashed curves): resonances $\nu_\theta : \nu_r = 3 : 1$ (left panel) and $\nu_{\rm K} : \nu_r = 3 : 1$ (right panel).

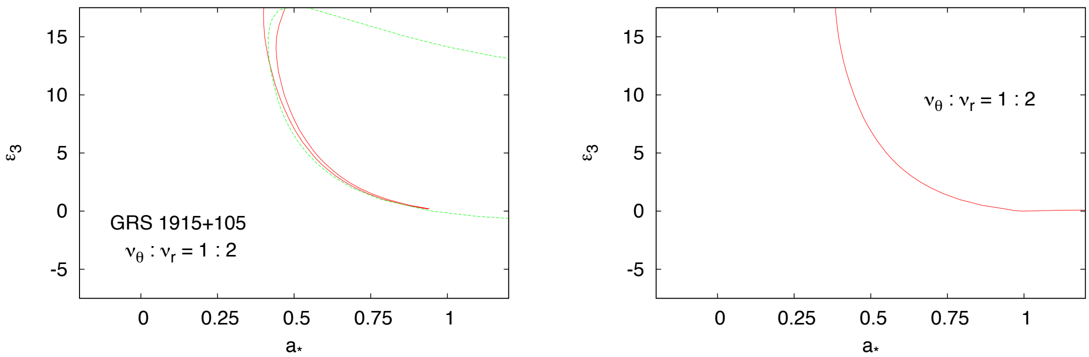

Figure 9. Left panel: as in Fig. 8, for the resonance $\nu_\theta : \nu_r = 1 : 2$. Right panel: boundary delimiting the JP space-times with and without the resonance $\nu_\theta : \nu_r = 1 : 2$; for $\epsilon_3 \le 0$, the resonance $\nu_\theta : \nu_r = 1 : 2$ is never possible, while for $\epsilon_3 > 0$ the resonance exists only for some values of the spin parameter (we notice that the red curve reaches a minimum at $a_* = 1$, where $\epsilon_3 \to 0^+$, and then goes up very slowly).

5 Discussion and conclusions

The high-frequency QPOs observed in some stellar-mass BH candidates may be used to test the Kerr-nature of these objects and to confirm, or rule out, the Kerr BH hypothesis. These frequencies are indeed almost constant, suggesting that their value is not determined by the properties of the fluid accretion flow, but by the geometry of the space-time. If we assume the stellar-mass BH candidates are the Kerr BHs predicted by General Relativity, the high-frequencies QPOs may be used to estimate the spin parameter. However, at least in the framework of the resonance models, the estimates of the spin parameter inferred from the observed QPOs of three micro-quasars seem not to be consistent with the measurements obtained from the analysis of the thermal spectrum of the disk of the same objects, in the sense it is not possible to explain the observations of all the three micro-quasar by invoking a unique mechanism for the production of the high-frequencies QPOs (actually, this assertion

remains true even in all the other models proposed so far in the literature). We have thus four possibilities: *i*) the resonance models are wrong, *ii*) the continuum-fitting method does not provide reliable estimate of a_*, *iii*) both techniques do not work correctly, *iv*) these objects are not Kerr BHs.

While systematic effects and/or wrong models are surely the most likely possibility to explain the disagreement between the two approaches, in this paper I explored the scenario *iv*) and I found two (speculative) explanations:

1. *All the observations can be explained with the resonance* $\nu_\theta : \nu_r = 3 : 1$. As we can see from the central left panel in Fig. 3 and the left panels in Figs. 7 and 8, the resonance $\nu_\theta : \nu_r = 3 : 1$ may explain the high-frequency QPOs of the three micro-quasars in agreement with the measurements obtained from the continuum-fitting method, at the price of a deformation parameter $\epsilon_3 \sim 5 - 15$; that is, these BH candidates should not be the Kerr BH predicted by General Relativity. GRO J1655-40 and XTE J1550-564 would be slow-rotating compact objects and the profile of the radial and the vertical epicyclic frequencies would be like the one in the right panel of Fig. 5; that is, the resonance $\nu_\theta : \nu_r = 3 : 1$ would be present at a unique radius $r_{3:1}$. GRS 1915+105 would instead be a "fast-rotating" object with $a_* \approx 0.5$ and the situation would be like the one in the left panel of Fig. 5: the resonance $\nu_\theta : \nu_r = 3 : 1$ is possible at two different radii, but we would observe the one occurring at the smaller one, which should indeed be expected to be stronger. Let us notice that the value $a_* \approx 0.5$ might be close to the maximum value of the spin parameter for a compact object with $\epsilon_3 \sim 5 - 15$, see Fig. 1 in Ref. [34]. For GRS 1915+105, the allowed region delimited by the green dashed line is likely in large part unphysical (equivalent to a Kerr metric with $|a_*| > 1$, i.e. it may be impossible to create such a fast-rotating objects) and therefore it is not so strange that the overlap between the bounds from the QPOs and the continuum-fitting method is a thin area near the boundary of the region allowed by the continuum-fitting method.

2. *The observed high-frequency QPOs are produced by different resonances determined by value of the the spin parameter of the compact object.* Unlike in the Kerr background, for non-Kerr metrics such a scenario is much more appealing because there are excitation modes possible only if the object has a spin parameter exceeding a critical value. So, for a given deformation parameter, the resonance responsible for the production of the high-frequency QPOs would be determined by the specific value of the spin parameter of the compact object. This possibility can be better understood with the following example. In the model briefly reviewed in Subsection 3.1, resonances are possible only for $\nu_r/\nu_\theta = 2/n$ with n integer. When $\nu_\theta > \nu_r$, the minimum n is 3. However, for $\epsilon_3 > 0$, the minimum value of n depends on the spin parameter a_*. For small value of the spin parameter, $n_{\rm min} = 3$, as in Kerr. Above a critical value of the spin parameter, which depends on ϵ_3, $n_{\rm min} = 1$ or 2. So, we may imagine a model in which GRO J1655-40 and XTE J1550-564 present the resonance $\nu_\theta : \nu_r = 3 : 1$, because their BH candidates are slow-rotating objects and $\nu_\theta > \nu_r$. On the other hand, for GRS 1915+105 even the resonances with $\nu_r > \nu_\theta$ could be excited, and actually be stronger. A deformation parameter $\epsilon_3 \sim 5 - 15$ is still required, i.e. the three micro-quasars should be objects more prolate than Kerr BHs.

The high-frequency QPOs are potentially an excellent tool to investigate the geometry of the space-time around stellar-mass BH candidates and to measure the fundamental properties

of these objects. For the time being, however, we do not know the exact origin of these QPOs and therefore any analysis depends on the assumed model. In this paper, I have considered the resonance models first proposed by Abramowicz and Kluzniak, because they have a number of nice features, and compared the results with the measurements of the thermal spectrum of the disk performed by the Harvard group. All the observations of the three micro-quasars for which we can do this test can be explained if we admit that these objects are not Kerr BHs. Within the theoretical framework proposed by Johannsen and Psaltis with a single deformation parameter, one finds that current data demand $\epsilon_3 \sim 5 - 15$, while a Kerr BHs would require $\epsilon_3 = 0$, and for $\epsilon_3 > 0$ (< 0) the gravitational force on the equatorial plane is weaker (stronger) than the one around a Kerr BH with the same mass and spin. At a speculative level, we can notice that this value of ϵ_3 is consistent with another non-zero measurement, $\epsilon_3 \approx 7.5$, found in Ref. [22]. The idea behind the work of Ref. [22] is that the steady jets observed in some micro-quasars may be powered by the Blandford-Znajek mechanism [64], which is one of the most appealing scenarios to explain this kind of phenomena. If this is the case, one should expect a correlation between the power of steady jets and the value of the spin parameter of the micro-quasars. Comparing current estimates of the jet power with the measurements of the spin parameter obtained by the continuum-fitting method, one finds there is no correlation if the micro-quasars are Kerr BHs, i.e. if $\epsilon_3 = 0$, but a correlation is possible, and actually close to the theoretical predictions $P_{\rm jet} \sim a_*^2$, for $\epsilon_3 \approx 7.5$ [22].

Acknowledgments

This work was supported by the Humboldt Foundation.

References

[1] B. Carter, Phys. Rev. Lett. **26**, 331 (1971).

[2] D. C. Robinson, Phys. Rev. Lett. **34**, 905 (1975).

[3] P. T. Chrusciel and J. Lopes Costa, arXiv:0806.0016 [gr-qc].

[4] R. Penrose, Riv. Nuovo Cim. **1**, 252-276 (1969).

[5] J. R. Oppenheimer and H. Snyder, Phys. Rev. **56**, 455 (1939).

[6] P. Pani, E. Barausse, E. Berti and V. Cardoso, Phys. Rev. D **82**, 044009 (2010) [arXiv:1006.1863 [gr-qc]].

[7] E. Barausse, V. Cardoso and G. Khanna, Phys. Rev. Lett. **105**, 261102 (2010) [arXiv:1008.5159 [gr-qc]].

[8] B. Giacomazzo, L. Rezzolla and N. Stergioulas, Phys. Rev. D **84**, 024022 (2011) [arXiv:1105.0122 [gr-qc]].

[9] P. S. Joshi and D. Malafarina, Phys. Rev. D **83**, 024009 (2011) [arXiv:1101.2084 [gr-qc]].

[10] P. S. Joshi and D. Malafarina, arXiv:1105.4336 [gr-qc].

[11] F. Caravelli, L. Modesto, Class. Quant. Grav. **27**, 245022 (2010). [arXiv:1006.0232 [gr-qc]].

[12] C. Bambi and L. Modesto, Phys. Lett. B **706**, 13 (2011) [arXiv:1107.4337 [gr-qc]].

[13] R. Narayan, New J. Phys. **7**, 199 (2005) [gr-qc/0506078].

[14] C. E. Rhoades and R. Ruffini, Phys. Rev. Lett. **32**, 324 (1974).

[15] V. Kalogera and G. Baym, Astrophys. J. **470**, L61 (1996).

[16] C. Bambi, Mod. Phys. Lett. A **26**, 2453 (2011) [arXiv:1109.4256 [gr-qc]].

[17] C. Bambi and E. Barausse, Astrophys. J. **731**, 121 (2011) [arXiv:1012.2007 [gr-qc]].

[18] S. Chen and J. Jing, Phys. Lett. B **711**, 81 (2012) [arXiv:1110.3462 [gr-qc]].

[19] A. C. Fabian, K. Nandra, C. S. Reynolds *et al.*, Mon. Not. Roy. Astron. Soc. **277**, L11 (1995).

[20] T. Johannsen and D. Psaltis, arXiv:1202.6069 [astro-ph.HE].

[21] C. Bambi, Phys. Rev. D **85**, 043002 (2012) [arXiv:1201.1638 [gr-qc]].

[22] C. Bambi, arXiv:1204.6395 [gr-qc].

[23] N. Wex and S. Kopeikin, Astrophys. J. **514**, 388 (1999) [arXiv:astro-ph/9811052].

[24] O. Dreyer *et al.*, Class. Quant. Grav. **21**, 787 (2004) [gr-qc/0309007].

[25] F. D. Ryan, Phys. Rev. D **52**, 5707 (1995).

[26] K. Glampedakis and S. Babak, Class. Quant. Grav. **23**, 4167 (2006) [arXiv:gr-qc/0510057].

[27] L. Barack and C. Cutler, Phys. Rev. D **75**, 042003 (2007) [arXiv:gr-qc/0612029].

[28] C. M. Will, Astrophys. J. **674**, L25 (2008) [arXiv:0711.1677 [astro-ph]].

[29] C. Bambi and K. Freese, Phys. Rev. D **79**, 043002 (2009) [arXiv:0812.1328 [astro-ph]].

[30] C. Bambi and N. Yoshida, Class. Quant. Grav. **27**, 205006 (2010) [arXiv:1004.3149 [gr-qc]].

[31] T. Johannsen and D. Psaltis, Astrophys. J. **718**, 446 (2010) [arXiv:1005.1931 [astro-ph.HE]]

[32] C. Bambi, F. Caravelli and L. Modesto, Phys. Lett. B **711**, 10 (2012) [arXiv:1110.2768 [gr-qc]].

[33] C. Bambi, Phys. Rev. D **83**, 103003 (2011) [arXiv:1102.0616 [gr-qc]].

[34] C. Bambi, Phys. Lett. B **705**, 5 (2011) [arXiv:1110.0687 [gr-qc]].

[35] M. Gierlinski, M. Middleton, M. Ward and C. Done, Nature **455**, 369 (2008) [arXiv:0807.1899 [astro-ph]].

[36] R. A. Remillard and J. E. McClintock, Ann. Rev. Astron. Astrophys. **44**, 49 (2006) [astro-ph/0606352].

[37] L. Stella and M. Vietri, Astrophys. J. **492**, L59 (1998) [astro-ph/9709085].

[38] L. Stella and M. Vietri, Phys. Rev. Lett. **82**, 17 (1999) [astro-ph/9812124].

[39] C. A. Perez, A. S. Silbergleit, R. V. Wagoner and D. E. Lehr, Astrophys. J. **476**, 589 (1997) [astro-ph/9601146].

[40] A. S. Silbergleit, R. V. Wagoner and M. Ortega-Rodriguez, Astrophys. J. **548**, 335 (2001) [astro-ph/0004114].

[41] R. V. Wagoner, A. S. Silbergleit and M. Ortega-Rodriguez, Astrophys. J. **559**, L25 (2001) [astro-ph/0107168].

[42] S. Kato, Publ. Astron. Soc. Jap. **53** 1 (2001).

[43] M. A. Abramowicz and W. Kluzniak, Astron. Astrophys. **374**, L19 (2001) [astro-ph/0105077].

[44] M. A. Abramowicz, V. Karas, W. Kluzniak, W. H. Lee and P. Rebusco, Publ. Astron. Soc. Jap. **55** 467 (2003).

[45] W. Kluzniak and M. A. Abramowicz, Astrophys. Space Science **300**, 143 (2005).

[46] G. Torok, M. A. Abramowicz, W. Kluzniak and Z. Stuchlik, Astron. Astrophys. **436**, 1 (2005).

[47] Z. Stuchlik and A. Kotrlova, Gen. Rel. Grav. **41**, 1305 (2009) [arXiv:0812.5066 [astro-ph]].

[48] A. N. Aliev, G. D. Esmer and P. Talazan, arXiv:1205.2838 [gr-qc].

[49] T. Johannsen and D. Psaltis, Astrophys. J. **726**, 11 (2011) [arXiv:1010.1000 [astro-ph.HE]].

[50] A. N. Aliev and A. E. Gumrukcuoglu, Phys. Rev. D **71**, 104027 (2005) [hep-th/0502223].

[51] G. Torok, A. Kotrlova, E. Sramkova and Z. Stuchlik, Astron. Astrophys. **531**, 59 (2011) [arXiv:1103.2438 [astro-ph.HE]].

[52] T. Johannsen and D. Psaltis, Phys. Rev. D **83**, 124015 (2011) [arXiv:1105.3191 [gr-qc]].

[53] C. Bambi and E. Barausse, Phys. Rev. D **84**, 084034 (2011) [arXiv:1108.4740 [gr-qc]].

[54] C. Bambi, Phys. Rev. D **85**, 043001 (2012) [arXiv:1112.4663 [gr-qc]].

[55] T. E. Strohmayer, Astrophys. J. **552**, L49 (2001) [astro-ph/0104487].

[56] R. A. Remillard, M. P. Muno, J. E. McClintock and J. A. Orosz, Astrophys. J. **580**, 1030 (2002) [astro-ph/0202305].

[57] C. Bambi, Europhys. Lett. **94**, 50002 (2011) [arXiv:1101.1364 [gr-qc]].

[58] C. Bambi, JCAP **1105**, 009 (2011) [arXiv:1103.5135 [gr-qc]].

[59] S. N. Zhang, W. Cui and W. Chen, Astrophys. J. **482**, L155 (1997) [astro-ph/9704072].

[60] L. -X. Li, E. R. Zimmerman, R. Narayan and J. E. McClintock, Astrophys. J. Suppl. **157**, 335 (2005) [astro-ph/0411583].

[61] J. E. McClintock, R. Narayan, S. W. Davis, L. Gou, A. Kulkarni, J. A. Orosz, R. F. Penna and R. A. Remillard *et al.*, Class. Quant. Grav. **28**, 114009 (2011) [arXiv:1101.0811 [astro-ph.HE]].

[62] J. E. McClintock, R. Shafee, R. Narayan, R. A. Remillard, S. W. Davis and L. -X. Li, Astrophys. J. **652**, 518 (2006) [astro-ph/0606076].

[63] M. Middleton, C. Done, M. Gierlinski and S. Davis, Mon. Not. Roy. Astron. Soc. **373**, 1004 (2006). [astro-ph/0601540].

[64] R. D. Blandford and R. L. Znajek, Mon. Not. Roy. Astron. Soc. **179**, 433 (1977).